GU J Sci, Part C, 11(1): 236-251 (2023)

Gazi University

Journal of Science

PART C: DESIGN AND TECHNOLOGY

http://dergipark.gov.tr/gujsc

Experimental investigation of engineering properties of silica sand filled mortars containing high doses of SWCNT

Fatih DOĞAN[1] Heydar DEHGHANPOUR[2,*] Serkan SUBAŞI[3] Muhammed MARAŞLI[2]

[1]*Munzur University, Rare Earth Elements Application & Research Center, Tunceli, Türkiye*

[2]*Fibrobeton Company, R&D Center, Düzce, Türkiye*

[3]*Department of Civil Engineering, Düzce University, Engineering Faculty, Düzce, Türkiye*

Article Info

Research article
Received:06/08/2022
Revision:19/12/2022
Accepted:29/12/2022

Keywords

Conductive Mortars
SWCNT
Resistivity
Damping Ratio
Steel Fiber

Abstract

Recently, great efforts have been made by researchers on the mixture of electrically conductive concretes that have been developed for different purposes. In this study, an experimental research was carried out on electrically conductive mortar mixtures especially for shell elements produced for building facade cladding. Six different mixtures were produced, including the non-conductive reference mixture. Single-walled carbon nanotube (SWCNT) was used as nano-sized conductive additive material. SWCNT was added at 0.2% and 0.3% of cement weight. Steel fiber (SF) was added to the same mixtures as another group at the rate of 4% by total weight. 2, 14, 28, 90 and 180 days electrical resistivities of the obtained conductive mortar samples were measured. As a non-destructive method, dynamic resonance testing was performed and the 28-day damping rates of the samples were determined. Ultrasonic pulse velocity (UPV) and Leeb hardness tests were performed, respectively, by using other non-destructive testing methods to obtain information about the internal structure voids and surface hardness of the samples. The internal microstructure morphologies of the composite materials were analyzed by SEM (Scanning Electron Microscope) characterization method. In addition, elemental occurrences in the samples were explained by elemental mapping. The crystal phase formations in the cement matrix were characterized by XRD (X-Ray Diffraction) analyzer. SWCNT, which causes low machinability and therefore internal structure voids, caused a decrease in compressive strength and flexural strength, as well as a significant increase in electrical conductivity. Addition of 0.3 SWCNT reduced the electrical resistance of the material up to 3154 Ω.cm.

1. INTRODUCTION

Crack formation, which causes a decrease in the strength of cement-based concrete, which is used as a construction building material, leads researchers to use various additives. Also, interest in studies to improve the mechanical properties of cementitious materials has increased [1]. To increase the strength of Portland cement, there are studies on the use of nanoscale materials that will reduce the porous structure of the material [2, 3]. Particularly, nanoparticle-containing components are included in the cement mixture for structures requiring high strength in building materials [4]. There is increasing interest in studies on conductive concrete, which is obtained by mixing the conductive component, cement materials and aggregate in a certain ratio. Carbon nanotubes (CNTs) are of interest to researchers as reinforcement materials in cementitious materials due to their high electrical conductivity and high mechanical properties [5]. Rocha et al. reported that CNTs added to the cement mixture at well below 1% increased the flexural strength of concrete up to 50%. In addition, it was stated that C-S-H, which is the main component of hydrated Portland cement, is at nanoscale. Thus, it is important to add carbon nanotubes to Portland cement to produce new concrete with superior properties [6]. CNTs, which are considered as alternatives to improve the mechanical and electrical properties of Portland cement, show superior performance even

*Corresponding author, e-mail: heydar.dehghanpour@yahoo.com
DOI:10.29109/gujsc.1158688

though they are used in small amounts in the cement mixture [7]. The preference of carbon nanotubes in cementitious structures is associated with high strength and high modulus of elasticity [8]. In different studies, it is stated that CNTs, which can be homogeneously dispersed in the cement matrix, prevent the growth of cracks that may occur in concrete [9–11]. Since high-strength cementitious materials exhibit brittle properties, it is stated that the addition of CNTs to the cement mixture provides an increase in flexural strength. Parveen et al. [12] reported that the mechanical and microstructural properties of the material were improved with the addition of CNTs to the cement mixture.

However, in this study, it is aimed to examine the relationship between mechanical strength and electrical resistance of the concrete to be produced by adding different reinforcement materials to the cement mixture, considering the studies made with CNTs, in comparison with the literature studies. Although there is more research on CNT reinforcement to strengthen concrete material, applications of single-walled carbon nanotube (SWCNT) and multi-walled carbon nanotube (MWCNT) are more preferred [13]. In the literature, it is stated that the SWCNT additive to the cement mortar better reflects the thermal properties of the material compared to MWCNT [14]. The fact that SWCNT is not preferred as much as MWCNT in building materials is stated as high cost and hydrophobic feature. To solve this problem, it has been explained that processes that facilitate the dispersion of SWCNT, which has a higher surface area, in the solution can be performed [15]. In addition, Hu et al. [16] reported that SWCNTs with high specific area contribute more to the increase in strength in cementitious mixtures compared to MWCNTs. Studies investigating the mechanical and electrical properties of SWCNT reinforced to the cement mixture in concrete production are limited. It has been reported by Makar and Chan [9] that SWCNT added to Portland cement improves the mechanical strength results of concrete. This is explained by the fact that SWCNT included in the cement mix accelerates the hydration process. Tyson et al. added dispersed SWCNT to the cement mixture and emphasized that the mechanical properties of the concrete were improved [17].

Adding fiber to the cement matrix prevents the formation of cracks in the concrete and the spread of cracks and contributes to the increase in the strength of the concrete [18]. Research has been carried out on the workability of concretes produced with the reinforcement of various fiber components. Fiber reinforced concrete significantly improves the mechanical properties of the material compared to normal concrete [19]. Among the fibers, steel fibers with high strength properties are preferred in industrial applications. In the study of Yazıcı et al. [20], it was reported that there was an improvement in the flexural strength of concrete reinforced with steel fiber. It has been stated that the steel fibers added to the cement paste increase the strength properties of the concrete and prevent the formation of cracks by reducing the porous structure [21]. The strength and ductility of concrete materials containing steel fiber are quite high compared to normal concrete [22]. In addition, the steel fibers dispersed in the cement matrix contribute to the damping of the impact energy under dynamic load [23]. In the literature, it has been explained that the steel fibers added to the cement paste form a dense structure by reducing the porous structure of the concrete [24]. It has been explained that by adding conductive steel fibers to the cement mixture, the fiber distribution in the matrix affects the electrical properties of the concrete [25]. Furthermore, in studies the performance of concretes containing CNT and fiber, it has been stated that the compressive strength of CNT/steel fiber reinforced concrete is higher than only CNT reinforced concrete [26, 27]. In the previous study, the resistivity of ferrochrome filled conductive mortars containing SWCNT-SF decreased to 1000 Ω.cm [28]. In addition, the resistivity of CF reinforced ferrochrome filled conductive mortars has been reported up to 200 Ω.cm [29].

In this study, the microstructure, strength, and electrical resistance performances of SWCNT/steel fiber reinforced concrete, which have not yet been studied in the literature, were researched. Also, the effects of dispersed SWCNT and steel fiber on the engineering properties of cement paste were investigated comparatively. It is aimed to improve the resistivity properties and improve the mechanical properties of SWCNT/steel fiber conductive concrete. Compressive strength, flexural strength, dynamic resonance, UPV, and Leeb hardness tests were performed to examine the effect on the mechanical behavior of cementitious materials containing SWCNT and steel fiber. Also, the effect of SWCNT on damping ratio was investigated by dynamic resonance tests. Scanning electron microscopy (SEM) was used to investigate the role of SWCNTs and steel fibers in increasing the fracture resistance of conductive concretes and to investigate the morphological properties of the fibers. To examine the effect of additive components added

to cement paste on the electrical conductivity performance of concrete, measurements were made at different time intervals.

2.MATERIALS AND METHODS

2.1. Material Properties

Silica sand was used as the fine aggregate material in the all mixtures. In the literature, there are studies on electrically conductive cementitious materials produced with silica aggregate [28, 29]. CEM II-42.5 R white cement, which is preferred in facade cladding, was used as binder. As a pozzolanic additive material, calcined kaolin was preferred in equal proportions in all mixtures. Previous studies have shown that calcined kaolin performs well when used with white cement [30, 31]. The particle size ranges of silica sand, cement and calcined kaolin were compared in Table 1. The SWCNT dispersed with the carboxy methyl cellulose agent used in the study was provided by TUBAL. The carbon content of the SWCNT used was 99 ± 1 wt% and had a diameter of 1 – 2 nm. The length of this material, which is very flexible and strong, is about 3000 times its diameter. Normal tap water was used as mixing water. Stainless steel fiber (SF) with a length of 12.5 mm and a diameter of 0.175 mm was preferred as conductive fiber in mixtures. Polycarboxylate based superplasticizer was used to ensure adequate workability in all mixtures. Details of conductive mortar mixtures are given in Table 2. Silica sand (SS) filled pure mixture is a normal premix mortar consisting of filler, binder, pozzolanic, water and plasticizer, and is defined as the matrix for other mixtures. In the premix mixture, all dry ingredients are put into the mixer, mixed for 90 seconds, then plasticizer is added together with water and mixed for 90 seconds again and placed in molds. In the mixtures containing SWCNT, the water of the solution with SWCNT was taken as the basis instead of mains water. In steel fiber mixtures, after all the components came together, when the matrix was ready, the fibers were added and mixed with a mixer for one minute.

Table 1. *Granulometry of aggregates, cement and calcined kaolin used.*

silica sand		*Cement*		*calcined kaolin*	
sieve size (µm)	*Passing (%)*	*sieve size (µm)*	*Passing (%)*	*sieve size (µm)*	*Passing (%)*
10	*3.49*	*2*	*6.54*	*10*	*67.11*
20	*5.9*	*3*	*11.59*	*20*	*90.57*
30	*9.76*	*4*	*15.88*	*30*	*99.32*
40	*12.33*	*5*	*19.25*	*40*	*100*
45	*12.97*	*6*	*22.1*	-	-
50	*13.3*	*7*	*24.86*	-	-
60	*13.51*	*8*	*27.81*	-	-
70	*13.51*	*9*	*31.07*	-	-
80	*13.51*	*10*	*34.66*	-	-
90	*13.51*	*20*	*76.9*	-	-
100	*13.51*	*30*	*97.35*	-	-
150	*14.7*	*40*	*100*	-	-
200	*23.53*	-	-	-	-
250	*39.2*	-	-	-	-
300	*56.01*	-	-	-	-
350	*70.45*	-	-	-	-
400	*81.46*	-	-	-	-
450	*89.16*	-	-	-	-
500	*94.13*	-	-	-	-
1000	*100*	-	-	-	-

Table 2. *Component ratios in electrically conductive mortars.*

No	Code	Silica sand (g)	Cement (g)	Calcined kaolin (g)	Water (g)	SF (%)	SWCNT (%)	Superplasticizer (g)
1	SS	1350	500	50	209	0	0	6
2	SS-SF	1270	500	50	209	4	0	6
3	SS-CNT0.2	1350	500	50	209	0	0.2	8.5
4	SS-CNT0.3	1350	500	50	209	0	0.3	10.5
5	SS-SF-CNT0.2	1270	500	50	209	4	0.2	8.5
6	SS-SF-CNT0.3	1270	500	50	209	4	0.3	10.5

2.2. Test methods

Within the scope of the study, non-destructive tests were carried out on 40 x 40 x 160 mm prismatic specimens without being subjected to destructive tests (compressive and flexural strength). Electrical resistivity measurement, ultrasonic pulse velocity (UPV), dynamic resonance and Leeb hardness tests were performed as non-destructive tests. Two-point uniaxial test method was used for electrical resistivity measurement. This method is also used frequently in the literature [32, 33]. In this method, a certain potential difference is applied between the two surfaces of the sample and the amount of current flowing is measured. Using ohm's law, the resistivity of the sample is obtained. A potential difference of 30V was used in all resistivity measurements. The frequency was fixed at 50 Hz during the resistiviti measurement. The UPV test was carried out to obtain information about the defects in the internal structure of the samples. In the UPV test, probes are placed on both sides of the sample. While one of the probes sounds, the other probe reads the elapsed time of the sound. The UPV value is obtained by dividing the sample length by the elapsed time. In the dynamic resonance test method, the sample was fastened in the midpoint between two supports and oscillation was applied from one end of the sample with a spherical impact pull, while the impact response from the other end was measured with an accelerometer. The damping ratio of the sample was determined according to the data obtained. Test setup images summarizing the all experimental procedure are shown in figure 1. UPV tests were performed according to ASTM C597 [34]. Longitudinal resonance frequency testing was performed for all samples according to ASTM C215 standard [35]. The ASTM A956 standard [36] was used to determine the Leeb hardness of the produced samples. Flexural and compressive strength tests were carried out in accordance with the TS EN 196-1 standard [37]. In addition, densities were calculated by measuring the dry weight and dimensions of all 28-day samples. Microstructural and morphological properties of SS, SS-CNT0.2 and SS-CNT0.3 samples were determined by SEM characterization tests. Also, the effect of adding a high amount of SWCNT to the conductive concrete on the elemental formations in the structure was investigated by EDS-mapping of the SS-CNT0.3 sample. In addition, the crystal phases of the SS, SS-CNT0.2 and SS-CNT0.3 samples were analyzed using X-ray diffractometry at a scan rate of 1°/min and a test range of 10°–70°.

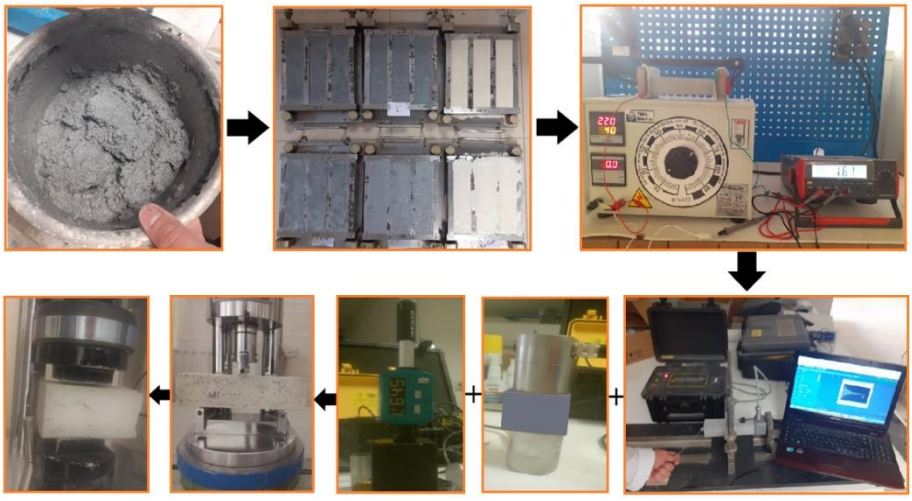

Figure 1. *Experimental flow view.*

3. RESULTS AND DISCUSSION

3.1. Electrical Resistivity

The electrical resistivity values of the mortar samples are summarized in figure 2. All values are calculated according to the amount of current obtained by applying a potential difference of 40 volts. Considering the 180-day resistivity results, it was determined that the resistivity value of the reference sample was 2-13 times higher than the resistivity values of the other mixtures. In addition, when the electrical resistivity values of all mixtures were examined according to the age of the sample, a decrease of approximately 9-22 times was observed between the values of 2 and 180 days. As can be seen from the figure, the difference in resistivity decreased in older ages. This may mean the complete disappearance of the internal water. The highest conductivity loss due to age was observed in the SS-SF sample as 22 times. While the 2-day resistivity value of this mixture was 939 Ω.cm, the 180-day resistivity value increased to 21300 Ω.cm. In this mixture, a remarkable conductivity value was read when the presence of hydration water in the mixture and the intrinsic conductivity of the steel fiber were combined in the first 2 days. However, the conductivity decreased as a result of the loss of water over time. Another important reason in this mixture is that the electrical current path is closed/decreased by coating the steel fibers with hydration products over time [32]. The electrical resistivity results of the mixtures with the addition of 0.2% and 0.3% carbon nanotubes for 180 days were decreased by 28% and 89%, respectively, when compared to the reference mixture. It can be said that this is entirely due to the conductivity effect of SWCNT itself. When the resistivity results of the 2-days 0.2% and 0.3% carbon nanotube added mixtures were examined, it decreased by 68% and 87%, respectively, when compared to the reference mixture. The point that draws attention here is that the resistivity of the mixture with 0.3% SWCNT changes very little over time. When SF was added to these two SWCNT added mixtures, the resistivity values were observed to decrease 7.4 and 12.9 times, respectively, compared to the reference sample. Steel fibers form a network within the matrix containing the SWCNT, both providing the current passing through it and reducing the resistivity of the matrix by connecting the SWCNTs to each other. The 180-day resistivity values obtained within the scope of the study were between 40557-3154 Ω.cm. The specification of a conductivity class for concretes may vary for different purposes. The electrical resistivity of the outdoor dried concrete was determined as 6.54 x 105–11.4 x 105 Ω.cm. In addition, according to studies conducted by different researchers, the electrical resistivity of saturated concrete and dry concrete were found to be 106 Ω.cm and 109 Ω.cm, respectively [38].

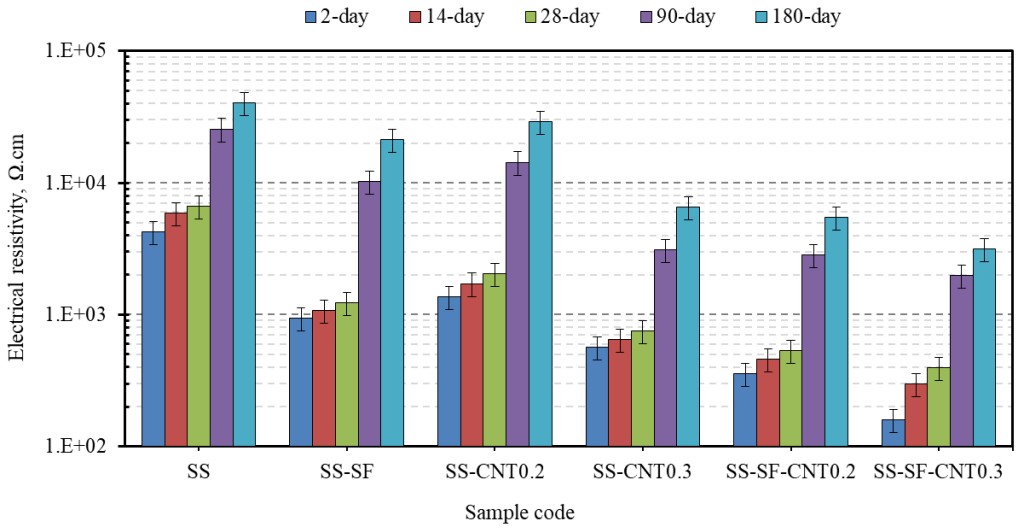

***Figure 2**. 2-180 Days electrical resistivity results of mortar specimens.*

3.2. Dynamic Resonance Test Results

The results of the dynamic resonance test, which is one of the important test methods for building materials within the scope of the study, are summarized in figure 3. In the figure, damping ratios are shown as balls and highlighted in the same color as the guide lines colored according to the sample codes. Amplitude curve was drawn in wide frequency range under the resonance test results, and damping ratios of all samples were

calculated accordingly. When the figure is examined in general, it is observed that the damping ratio values increase as the amplitude curves become horizontal. In the literature [39], high-narrow amplitude curves correspond to low damping ratio and low-wide curves correspond to high damping ratio. Considering the damping ratio values, it was observed that the damping property increased with the addition of steel fiber and SWCNT. The highest damping ratio was obtained for the SS-SF-CNT0.2 sample as 11%. The damping ratio of this sample improved as 84.40% compared to the reference (SS) sample. The damping ratio of the SS-SF sample containing 4% SF increased by 52.8% compared to the reference. Also, the damping rate of the samples containing 0.2% and 0.3% SWCNT improved 42.5% and 22%, respectively, compared to the reference. However, damping ratios of SS-CNT0.2 and SS-SF-CNT0.3 samples were obtained as equal. Luo et al. [40] in their study on cementitious composites containing carbon nanotubes, they emphasized that carbon nanotubes act as bridging microcracks, increase the interfacial "stick-slip" capacity and therefore improve the damping ratio. Also, in a previous study [41] on UHPCs, positive effects on the damping ratio of steel fiber were proven.

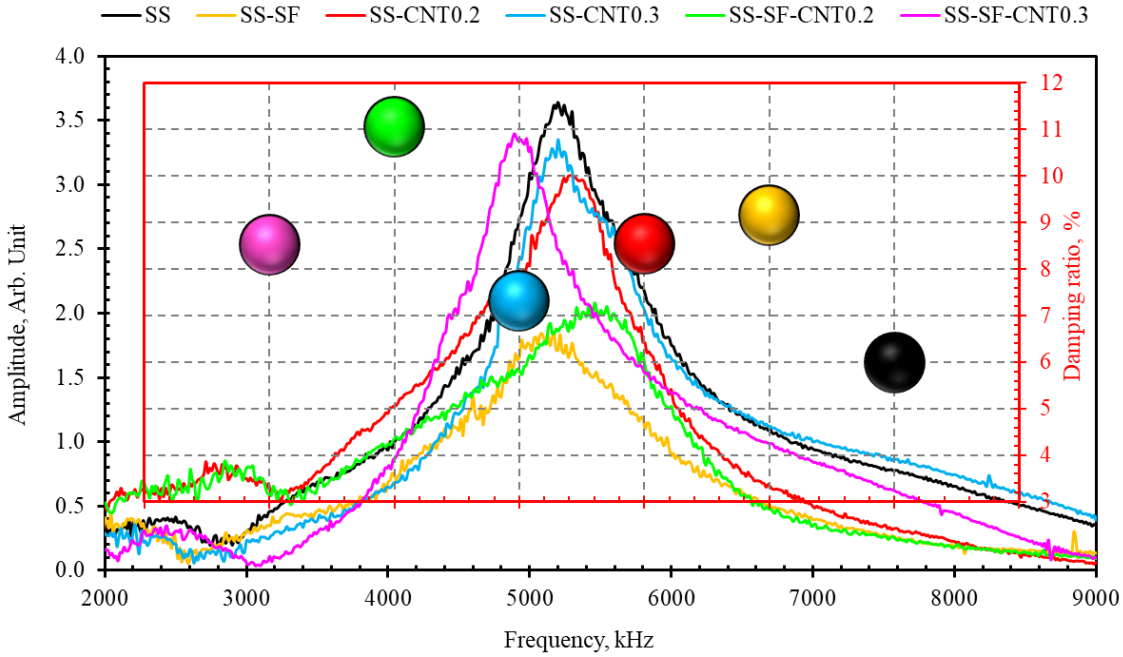

***Figure 3**. Dynamic resonance test results.*

3.3. Ultrasonic Pulse Velocity

When the UPV values are examined, it is observed that they are mostly in a parallel relationship with the density values. The UPV test method, known as the nondestructive method, is a technique used to determine the estimated compressive strength of building materials. UPV refers to the time it takes for the ultrasonic pulse to transfer a certain distance along the material, usually in concrete and mortar samples. In addition, internal defects such as porosity, microcracks and voids can also be detected by UPV testing. Therefore, it is possible to obtain information about the homogeneity of the material by performing the UPV test [42]. In order to obtain information about the internal structure defects of the samples produced in this study, UPV tests were performed and their dry densities were calculated. The results are summarized and compared in figure 4. Also, the linear relationship between UPV and density is given in figure 5. When the correlation coefficient between them was examined, a strong parallelism was observed. This is proof that the UPV values are directly related to the sample porosity ratio. Only the UPV value of the SS-SF sample decreased compared to the SS, while the density value increased. The UPV reduction in this mixture was 6.04%. Since the unit weight of steel fiber is about 4 times higher than the mortar, an increase in the density of the mortar with steel fiber addition can be observed, but the voids that occur in the mortar may cause a decrease in the ultrasonic transmission velocity. In the previous study [41], an increase in density and a decrease in UPV were observed in cementitious products with steel fiber added. The UPV values of the SS-CNT0.2 and SS-CNT0.3 mixtures decreased by 18% and 32%, respectively, compared to the reference.

SS-CNT0.3 had the lowest UPV and density values among the samples. Therefore, except for electrical conductivity, other properties such as mechanical and physical are expected to weaken.

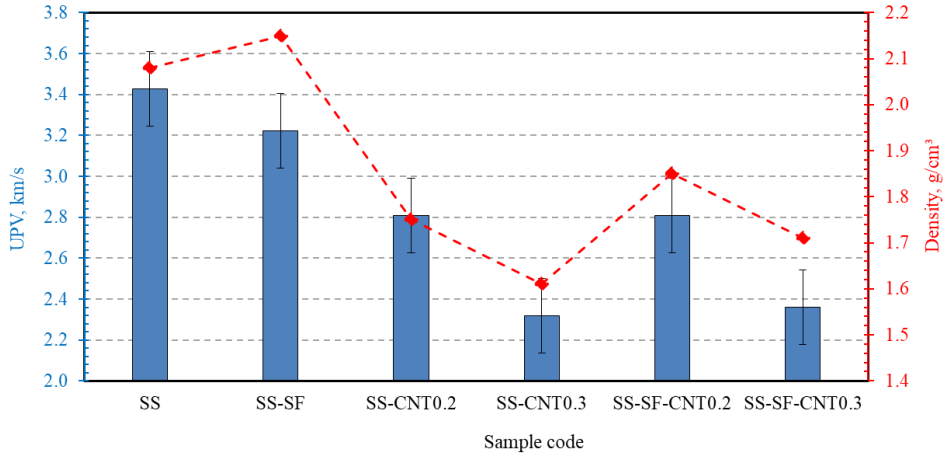

Figure 4. *UPV test results and density values of specimens.*

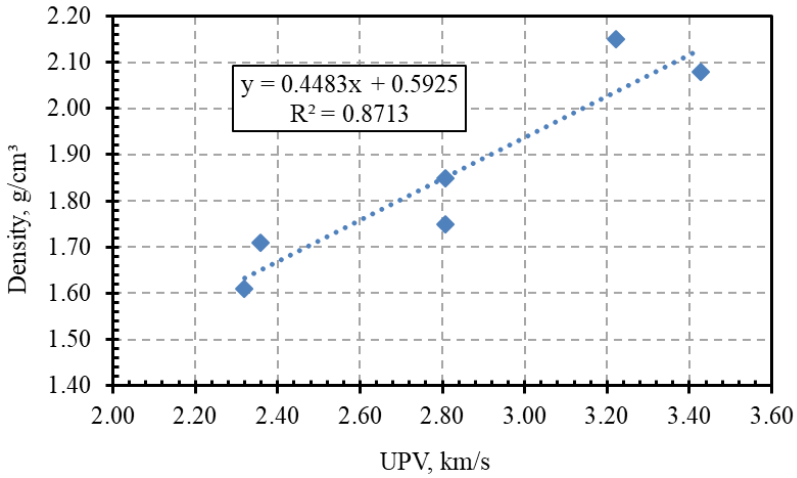

Figure 5. *Relationship between UPV and Density values.*

3.4. Leeb Hardness Results

Leeb hardness test was applied to obtain information about the surface hardness of the conductive mortar samples and the results are shown in figure 6. Leeb hardness value of SS-SF sample increased by 8.25% compared to SS. The reason for this is that steel fibers not only form a network in the mortar mixture, but also create a texture on the sample surface, increasing its hardness. The hardness values of SS-CNT0.2, SS-CNT0.3, SS-SF-CNT0.2 and SS-SF-CNT0.3 samples decreased by 15.13%, 28.90%, 9.48% and 22.21%, respectively, compared to the SS reference sample. With the addition of SWCNT, serious decreases were observed in the hardness values as well as the UPV values of the mixtures. This is entirely related to void formation due to low workability. Despite all these, the hardness values were obtained as 365-555 within the scope of the study.

There are a few Leeb hardness studies on normal concretes, although limited. Song et al. [43] investigated the Leeb hardness of sodium silicate based concrete and normal C30 concrete and concluded that the average hardness value of normal concrete was 362 HL and that of sodium silicate based concrete was 405 HL. The hardness values of the 28-day GRC specimens produced in this study were measured between 509 and 548 HL. Therefore, the results prove to be compatible when compared to normal concrete. The 2 and 7 day Leeb hardness results were measured as 396-438 and 456-510, respectively. Gomez-Heras et al. [44] stated that the finer the grain size, the higher the Leeb hardness. This situation is directly related to the filling of fine-grained minerals into micro and macro pores [45]. However, since the ratio of nano-sized SWCNT used in this study was higher than necessary and the presence of carboxymethyl cellulose as a

carrier material also caused defects in the mixture. Leeb hardness values were also low due to the imperfections.

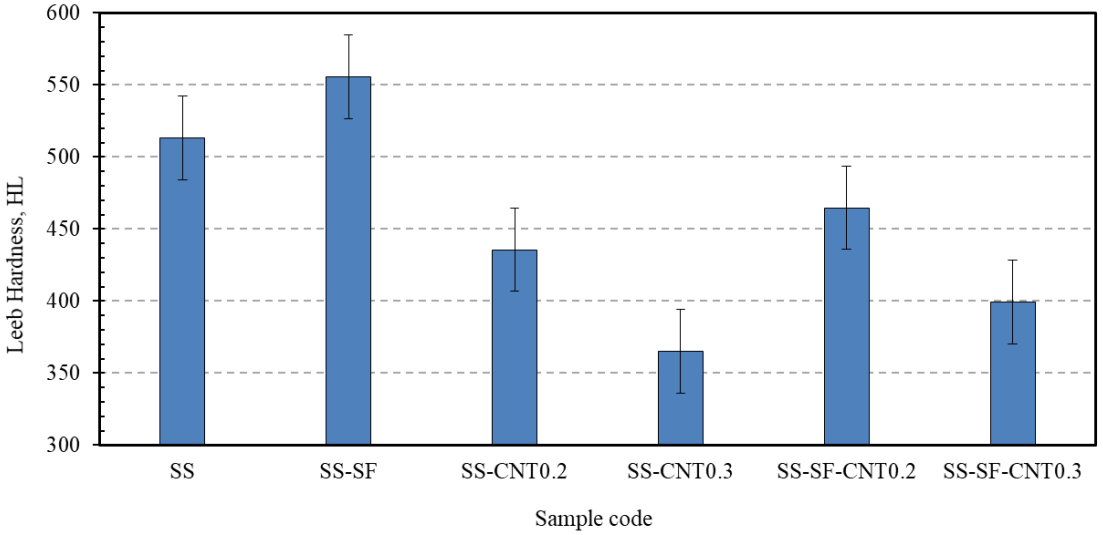

Figure 6. *Leeb hardness values of conductive mortars.*

3.5. Mechanical Test Results

The compressive and flexural strength results of conductive mortars containing carbon nanotubes are compared in figure 7. It is noteworthy that the strength of the mixtures decreased with the addition of SWCNT. However, considering the electrical resistivity results, the strength values were at an acceptable level considering the purpose of the study. The reason for the decrease in strength of SWCNT added mixtures is that the carbon nanotube has a high interfacial area, leading to low machinability and the formation of a more defective structure. In addition, the high concentration of carboxymethyl cellulose used as a dispersing agent in the SWCNT solution may leave permanent voids in the internal structure of the mortar, causing a decrease in strength. On the other hand, since the aim of this study was to design a conductive mortar mix, the SWCNT ratio was kept above the literature, which may decrease the strength by causing low adherence between the filler and the binder in the mixture. Studies [31, 46], have reported improvements in the strength of cementitious materials using lower dosages of SWCNT.

The compressive strengths of the mixtures containing 0.2% and 0.3% SWCNT decreased by 41.5% and 57.8%, respectively, compared to the reference sample. When 4% SF was added to the same mixtures, the decrease in strength was 30.3% and 52.1% compared to the reference. In addition, the compressive strength of the mixture containing only 4% SF increased by 17.4% compared to the reference. When the flexural strength results are examined, it is understood from both figure 7 and figure 8 that the values are in a parallel relationship with the compressive strength results. The flexural strength of the SF added mixture increased by 61.4% compared to the reference sample. The flexural strengths of the 0.2% and 0.3% SWCNT added mixtures decreased by 21.1% and 34.7%, respectively. The flexural strength of the mixture with 0.2% SWCNT and 4% SF increased by 26.3%. Also, the flexural strength of the mixture with 0.3% SWCNT and 4% SF was decreased by 26.3% compared to the reference. As a result, the decrease in compressive and flexural strengths may be related to the high SWCNT ratio. [47] Kang et al. investigated the strength of SWCNT-added cement composites at 0, 0,02, 0,04 and 0,06 wt% (based on cement weight). The positive effect of SWNT was observed in mixtures using dispersion additive. The maximum compressive strength was obtained for the composite containing 0.06% by weight of SWCNT. While Musso et al. [48] reported that functionalized CNTs had a negative effect on mechanical properties, they reported a significant improvement with both grown and annealed CNTs.

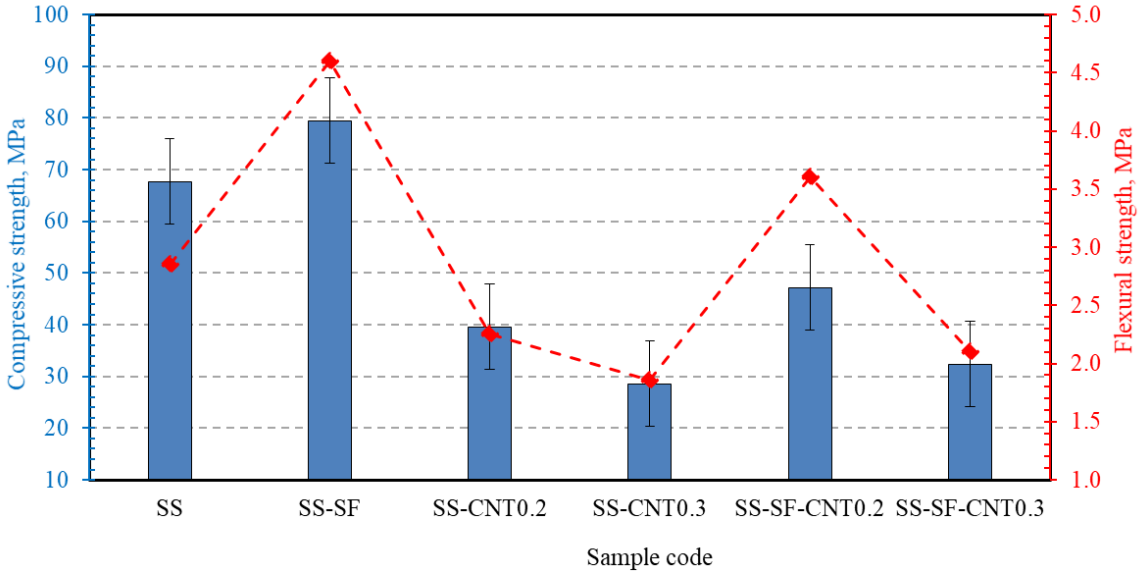

***Figure 7**. Compressive and flexural strength results.*

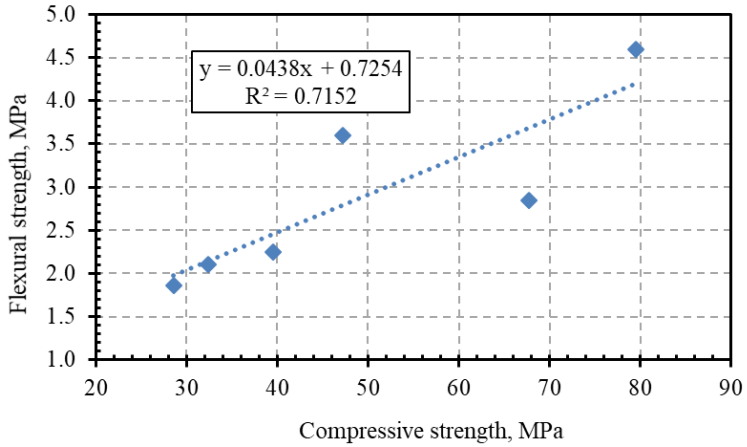

***Figure 8.** Linear relationship between compressive and flexural strengths.*

3.6. Microstructure Analysis Results

Microstructure pictures of silica sand characterized by SEM at different magnifications are shown in figure 9. In figure 9 (a), it is seen that silica sand particles form a high-density structure. On the other hand, it was observed that air voids were formed in the microstructure. It can be stated that SiO_2, which is the main component of silica sand, provides a high level of binding in the cement mixture and influences the strength values of the concrete sample (figure 9 (b)). It is understood that the intertwined SiO_2 particles have irregular shapes. The non-homogeneity of the particles can be attributed to the interparticle Van-der-Waals force and the tendency of the particles to agglomerate as reported by Saleh et al. [49]. The lack of porous structures in the morphology of the SS sample in high magnification SEM images (fig. 9 (c) and (d)) may be associated with $Ca(OH)_2$ in the mixture. The presence of C-S-H gel formed by the hydration reaction was determined. Thus, it can be said that C-S-H formations are effective on the compressive and flexural strengths of the SS concrete sample. The association of C-S-H formations with high compressive strength can be attributed to the bond strength of the particles in the mixture. It is reported that silica sand fills the pores by reducing the $Ca(OH)_2$ components and transforms the $Ca(OH)_2$ crystals of silica sand into C-S-H structure [49]. In addition, the ratio of silica sand in the cement mixture of the SS sample prevented the increase in the pore size in the matrix and contributed to the formation of dense structure. Furthermore, Huynh et al. [50] reported that the silica content in the cement paste prevented the formation of cracks in the concrete sample. Accordingly, the absence of cracked structures in the SEM images of the silica sand filled SS sample can be attributed to the silica content in the cement mixture.

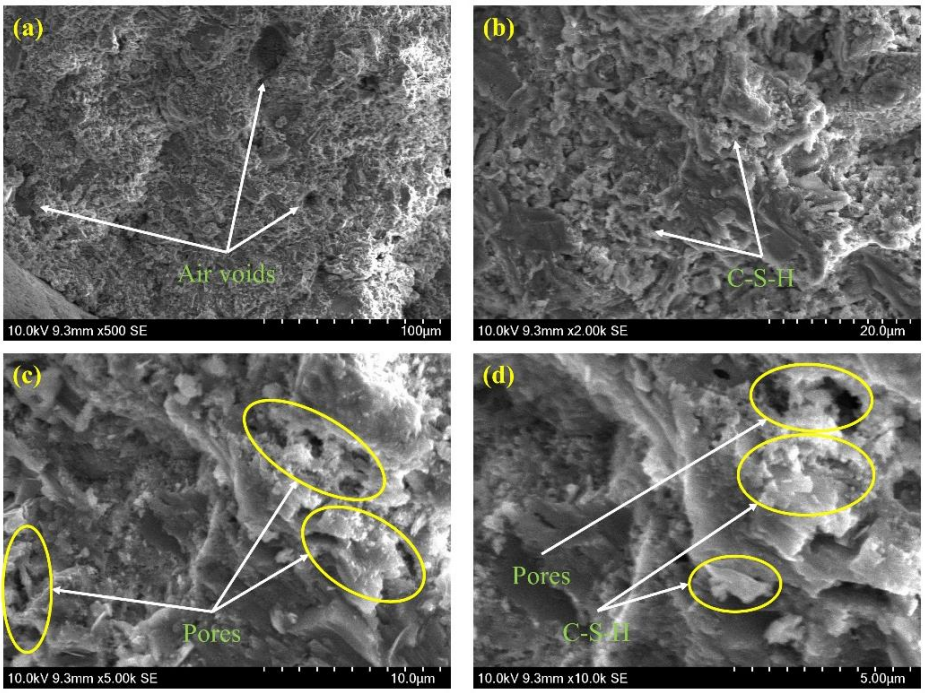

Figure 9. *SEM images of SS sample at different magnifications.*

SEM images of the conductive concrete sample containing 0.2% by weight of SWCNT at different magnifications are shown in figure 10. The low magnification SEM image shows micro-crack formation in the cement matrix (figure 10 (a)). The resulting micro-crack can be associated with the decrease in compressive and flexural strength values of 0.2% SWCNT added to the silica filled concrete mortar. C-S-H gel formations seen in figure 10 (b) morphology contributed to the compact structure in the sample. However, it can be said that the ettringite formations shown in the yellow dashed circle have a negative effect on the strength of the cement mortar. The enlarged SEM picture of the yellow dashed circle in figure 10 (b) is shown in figure 10 (c). It is seen that ettringite phases are formed clearly. The magnified SEM morphology of figure 10 (c) shows prominent ettringite formations and SWCNTs shown in the red dashed circle (figure 10 (d)). It can be noted that SWCNTs dry conductive network forming electrical conductivity between components in cement mortar [14]. In addition, the C-S-H formations shown in the red dashed circle and the SWCNT fibers interlocked to form a compact structure.

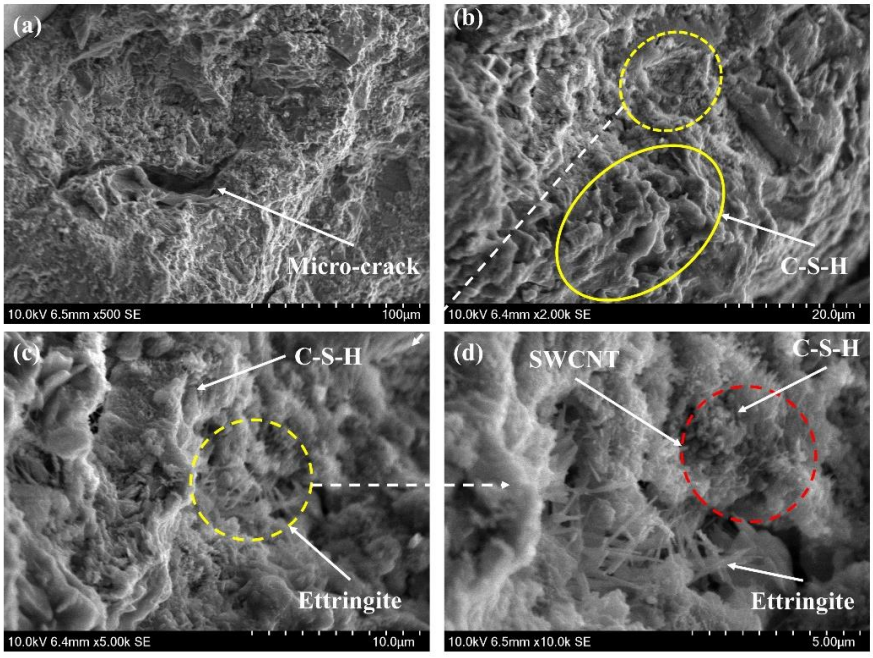

Figure 10. *Microstructure of SS-CNT0.2 conductive concrete sample at different magnifications.*

Figure 11 shows SEM images of a 0.3% SWCNT reinforced silica-filled cement mortar sample at different magnifications. As in the morphology picture of SS-CNT0.2 sample with 0.2% SWCNT additive, micro-crack formation is observed in the low-magnification SEM image of SS-CNT0.3 sample. In the SS-CNT0.3 sample, voids were formed in the morphology due to the increase in the amount of reinforcement component added to the cement mortar. The voids formed by the increase in the SWCNT content in the mixture caused the above-mentioned compressive and flexural strength values to decrease compared to the SS-CNT0.2 sample. It is seen that ettringite occurrences increase along the morphology in figure 11 (b). In addition, the presence of C-S-H products, which contribute to the increase in density in the microstructure, prevented a serious decrease in the strength values of concrete. Moreover, the CMC component shown in the green circle in figure 11 (b) improved the adhesion of the products in the cement mixture. Figure 11 (c) shows SWCNT fibers as well as C-S-H and ettringite components. In addition, it is seen that the SWNT fibers shown in the blue circle act as a bridging link between the hydration products. A high-magnification SEM image of the region shown in the black dashed circle in figure 11 (c) is given in figure 11 (d). Ettringite and C-S-H products are more prominent. In addition, the SWCNT fibers are seen to be clearer in the high magnification image and it has been confirmed that it forms conductive bonds between the hydration products. Nguyen et al. [5] reported that the fibers in the cement matrix effectively bond with the hydration products. Although the mechanical properties decrease with the increase in the SWCNT content added to the cement mixture in the above-mentioned strength test results, it can be said that SWCNT fibers contribute to the strength of the SS-CNT0.3 conductive concrete sample and improve its electrical conductivity properties. Furthermore, as stated by Hu et al. [16], very few SWCNTs in porous areas and their scattered clusters in the matrix caused a decrease in the mechanical strength of the SS-CNT0.2 sample.

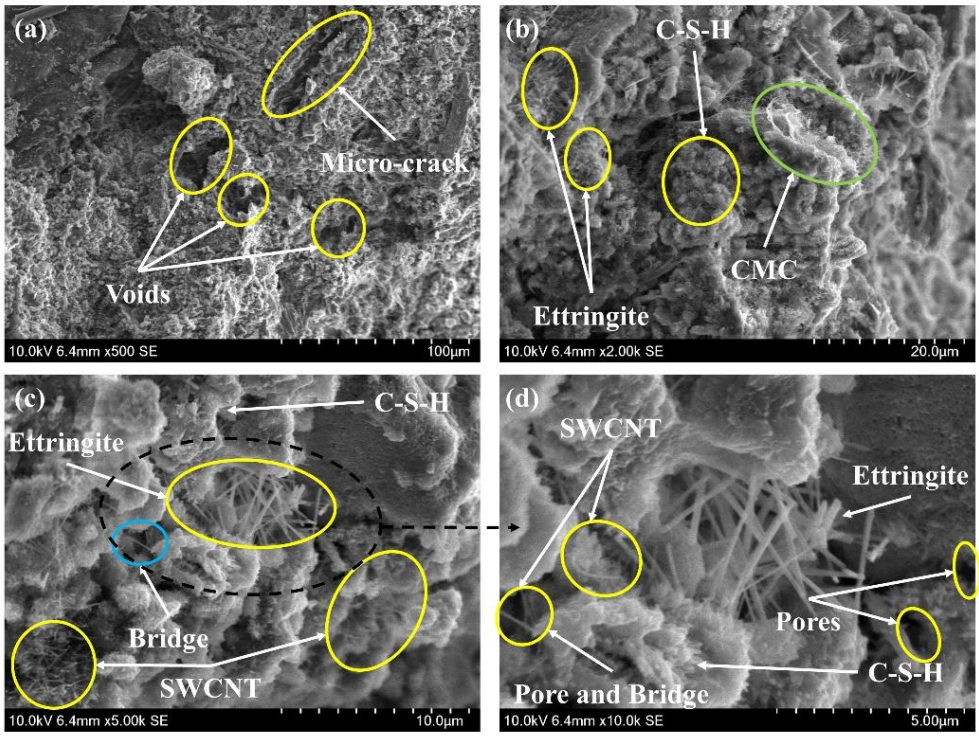

Figure 11. *Microstructure of SS-CNT0.3 conductive concrete sample at different magnifications.*

Figure 12 shows the elemental analysis results of the EDS mapping process taken from the low magnification SEM image of the SS-CNT0.3 sample. Calcium (Ca), oxygen (O), carbon (C), silicon (Si) and magnesium (Mg) elements were detected in the EDS mapping of the 0.3% SWCNT supplemented sample. It is seen that silica sand and cement mortar are dispersed in every region of the sample. The homogeneous distribution of Ca and Si elements constituting the C-S-H component in the mapped microstructure can be attributed to its contribution to improving the compactness of the sample structure. The porous structures are seen in the black circles in the EDS mapping image shown in figure 12 (b). When the distribution of the carbon element in figure 12 (c) is examined on the mapping, it is seen that the mapping in figure 12 (b) does not exist in the porous structures. Thus, it can be said that the SWCNT fibers in the matrix are not very effective in closing the gaps in the morphology and as a result, they do not provide

the desired contribution to the mechanical properties of the concrete sample. On the other hand, it can be stated that the distribution of the carbon element throughout almost the entire morphology in EDS mapping contributes to the resistance reduction of the conductive concrete sample by forming a conductive network between the cement matrix components of the SWCNTs.

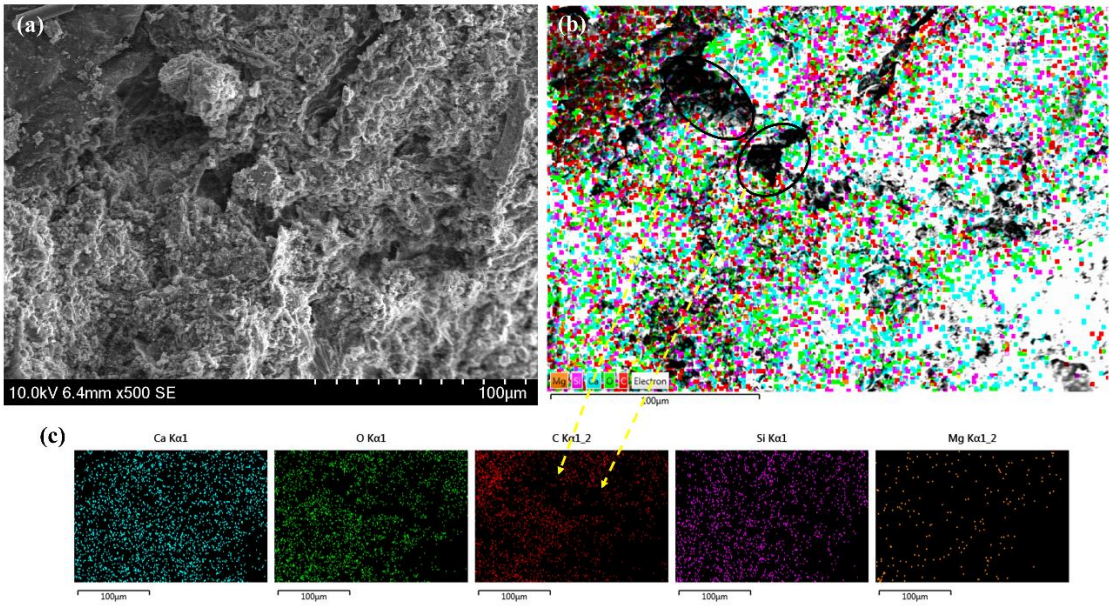

Figure 12. *Elemental mapping of SS-CNT0.3 sample.*

XRD patterns of SS, concrete sample is presented in the figure 13 quartz, calcite, and C_3S phases were formed in the X-ray diffraction patterns of the SS sample. The compact structure formed by the hydration products described in the SEM analysis of the SS sample in the sample morphology can be associated with the crystal phases detected in the XRD analysis of the SS sample. In addition, it can be said that the silica sand in the SS sample has an improving effect on the mechanical properties of the concrete sample by affecting the microstructure in the cement mixture. C3S phase was formed with the hydration of minerals that harden the cement. It is seen that the crystals formed because of hydration are compatible with the SEM analysis results and these crystals have contributed to the strength of the concrete sample by filling the voids in the microstructure [49]. On the other hand, carbon, C_3S, ettringite, portlandite phases are seen in the XRD analyzes of the conductive component samples produced with 0.2% and 0.3% SWCNT added to the SS sample. As seen in figure 13, the higher carbon peak intensity in the SS-CNT0.2 sample compared to the SS-CNT0.3 sample may be associated with the agglomeration of SWCNTs in the matrix. However, the higher C_3S and portlandite peak intensities in the SS-CNT0.3 sample compared to the SS-CNT0.2 sample confirms that the high SWCNT content in the cement mixture causes agglomeration in the matrix and the hydration products are dominant in the matrix. In addition, the reduction of calcite phases in the SS-CNT0.2 and SS-CNT0.3 samples can be attributed to the improvement of the structural properties of the samples [51].

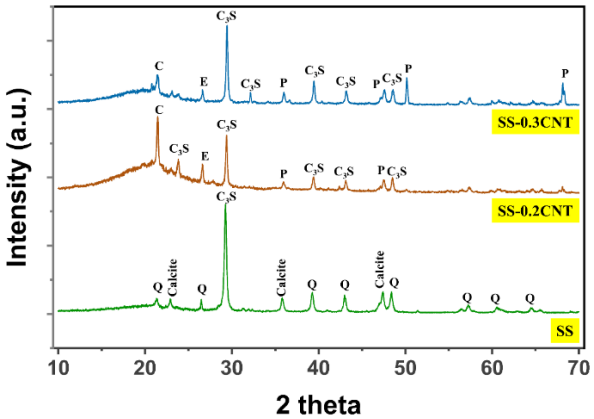

Figure 13. *XRD patterns of SS, SS-CNT0.2 and SS-CNT0.3 conductive concrete samples.*

4.CONCLUSIONS

While electrical resistivity values increased rapidly in the first ages, the rate of increase decreased in advanced ages. The reason for this was the drying of the samples and the loss of water in their bodies over time. A positive effect of SWCNT on conductivity was observed, but more reasonable results were obtained when used with SF. According to the dynamic resonance test results, SWCNT and SF caused the damping ratio to improve. Proving each other, the UPV, Leeb hardness and density values decreased with the addition of SWCNT. This was due to void formation due to low machinability. The compressive and flexural strengths of mixtures containing only carbon nanotubes were significantly reduced compared to the reference sample, but the addition of steel fiber slightly improved the values. In SEM morphology analysis, it has been reported that the particles in the SS sample have irregular shapes and the particles form a compact structure by intermingling with each other. It was observed that the pore size increased, and crack formation was prevented in the microstructure of the SS sample, depending on the silica sand ratio. In the SEM images of CNT reinforced silica sand samples (SS-CNT0.2 and SS-CNT0.3), it was stated that the SWCNT fibers in the cement matrix contributed to the reduction of the electrical resistance of the sample by establishing a conductive bond between the hydration products. However, the SWCNT in the cement mixture was not very effective in improving the strength properties of the concrete sample due to poor bridging function in the matrix porous structures. Although the SWCNTs were not fully active in the porous structures in the EDS-mapping analysis, their distribution in morphology improved the electrical conductivity of the sample. The crystalline phases in the structure were determined by X-ray analysis of SS, SS-CNT0.2 and SS-CNT0.3 samples. Accordingly, it was understood that the microstructures in the SEM characterizations and the XRD results were compatible with each other. It has been explained that the carbon peak intensities determined in the XRD phase analyzes of the samples containing SWCNT in the cement mixture are effective on the strength and conductivity of the concrete sample.

ACKNOWLEDGEMENTS

This study was carried out within the scope of the project coded STB-072161 of Fibrobeton R&D Center. Thank you to Fibrobeton Company for their support. We also thank Eti Krom Inc. for their support of olivine materials.

REFERENCES

[1] Nežerka, V., Bílý, P., Hrbek, V., & Fládr, J. (2019). Impact of silica fume, fly ash, and metakaolin on the thickness and strength of the ITZ in concrete. Cement and Concrete Composites, 103, 252–262.

[2] Zhan, B. J., Xuan, D. X., & Poon, C. S. (2019). The effect of nanoalumina on early hydration and mechanical properties of cement pastes. Construction and Building Materials, 202, 169–176.

[3] Rupasinghe, M., San Nicolas, R., Mendis, P., Sofi, M., & Ngo, T. (2017). Investigation of strength and hydration characteristics in nano-silica incorporated cement paste. Cement and Concrete Composites, 80, 17–30.

[4] Zhou, C., Li, F., Hu, J., Ren, M., Wei, J., & Yu, Q. (2017). Enhanced mechanical properties of cement paste by hybrid graphene oxide/carbon nanotubes. Construction and Building Materials, 134, 336–345.

[5] Nguyen, T. N. M., Yoo, D.-Y., & Kim, J. J. (2020). Cementitious material reinforced by carbon nanotube-Nylon 66 hybrid nanofibers: Mechanical strength and microstructure analysis. Materials Today Communications, 23, 100845.

[6] Gopalakrishnan, K., Birgisson, B., Taylor, P., & Attoh-Okine, N. O. (Eds.). (2011). Nanotechnology in Civil Infrastructure. Berlin, Heidelberg: Springer Berlin Heidelberg.

[7] Danoglidis, P. A., Konsta-Gdoutos, M. S., Gdoutos, E. E., & Shah, S. P. (2016). Strength, energy absorption capability and self-sensing properties of multifunctional carbon nanotube reinforced mortars. Construction and Building Materials, 120, 265–274.

[8] Zheng, L. X., O'Connell, M. J., Doorn, S. K., Liao, X. Z., Zhao, Y. H., Akhadov, E. A., … Zhu, Y. T. (2004). Ultralong single-wall carbon nanotubes. Nature Materials, 3(10), 673–676.

[9] Makar, J. M., & Chan, G. W. (2009). Growth of Cement Hydration Products on Single-Walled Carbon Nanotubes. Journal of the American Ceramic Society, 92(6), 1303–1310.

[10] Raki, L., Beaudoin, J., Alizadeh, R., Makar, J., & Sato, T. (2010). Cement and Concrete Nanoscience and Nanotechnology. Materials, 3(2), 918–942.

[11] Konsta-Gdoutos, M. S., Metaxa, Z. S., & Shah, S. P. (2010). Highly dispersed carbon nanotube reinforced cement based materials. Cement and Concrete Research, 40(7), 1052–1059.

[12] Parveen, S., Rana, S., Fangueiro, R., & Paiva, M. C. (2015). Microstructure and mechanical properties of carbon nanotube reinforced cementitious composites developed using a novel dispersion technique. Cement and Concrete Research, 73, 215–227.

[13] Abu Al-Rub, R. K., Ashour, A. I., & Tyson, B. M. (2012). On the aspect ratio effect of multi-walled carbon nanotube reinforcements on the mechanical properties of cementitious nanocomposites. Construction and Building Materials, 35, 647–655.

[14] Lee, H., Kang, D., Kim, J., Choi, K., & Chung, W. (2019). Void detection of cementitious grout composite using single-walled and multi-walled carbon nanotubes. Cement and Concrete Composites, 95, 237–246.

[15] Kim, J.-H., Choi, I.-J., & Chung, C.-W. (2021). Dispersion of single wall carbon nanotube using air entraining agent and its application to portland cement paste. Construction and Building Materials, 302, 124421.

[16] Hu, T., Jing, H., Li, L., Yin, Q., Shi, X., & Zhao, Z. (2019). Humic acid assisted stabilization of dispersed single-walled carbon nanotubes in cementitious composites. Nanotechnology Reviews, 8(1), 513–522.

[17] TYSON, B. M. (2012). Carbon nanotube and nanofiber reinforcement for improving the flexural strength and fracture toughness of Portland cement paste. Doctoral dissertation, Texas A & M University.

[18] Brandt, A. M. (2008). Fibre reinforced cement-based (FRC) composites after over 40 years of development in building and civil engineering. Composite Structures, 86(1–3), 3–9.

[19] Ryu, G. S., Kim, S. H., Ahn, G. H., & Koh, K. T. (2012). Evaluation of the Direct Tensile Behavioral Characteristics of UHPC Using Twisted Steel Fibers. Advanced Materials Research, 602–604, 96–101.

[20] Yazıcı, Ş., İnan, G., & Tabak, V. (2007). Effect of aspect ratio and volume fraction of steel fiber on the mechanical properties of SFRC. Construction and Building Materials, 21(6), 1250–1253.

[21] Kakooei, S., Akil, H. M., Jamshidi, M., & Rouhi, J. (2012). The effects of polypropylene fibers on the properties of reinforced concrete structures. Construction and Building Materials, 27(1), 73–77.

[22] Su, Y., Li, J., Wu, C., Wu, P., & Li, Z.-X. (2016). Effects of steel fibres on dynamic strength of UHPC. Construction and Building Materials, 114, 708–718.

[23] Liang, X., & Wu, C. (2018). Investigation on Thermal Conductivity of Steel Fiber Reinforced Concrete Using Mesoscale Modeling. International Journal of Thermophysics, 39(12), 142.

[24] Liang, X., & Wu, C. (2018). Meso-scale modelling of steel fibre reinforced concrete with high strength. Construction and Building Materials, 165, 187–198.

[25] Van Damme, S., Franchois, A., De Zutter, D., & Taerwe, L. (2004). Nondestructive determination of the steel fiber content in concrete slabs with an open-ended coaxial probe. IEEE Transactions on Geoscience and Remote Sensing, 42(11), 2511–2521.

[26] Lee, S. H., Kim, S., & Yoo, D.-Y. (2018). Hybrid effects of steel fiber and carbon nanotube on self-sensing capability of ultra-high-performance concrete. Construction and Building Materials, 185, 530–544.

[27] Park, H. M., Kim, G. M., Lee, S. Y., Jeon, H., Kim, S. Y., Kim, M., … Yang, B. J. (2018). Electrical resistivity reduction with pitch-based carbon fiber into multi-walled carbon nanotube (MWCNT)-embedded cement composites. Construction and Building Materials, 165, 484–493.

[28] DEHGHANPOUR, H., DOĞAN, F., SUBAŞI, S., & MARAŞLI, M. (2022). Effects of single-walled carbon nanotubes and steel fiber on recycled ferrochrome filled electrical conductive mortars. Journal of Sustainable Construction Materials and Technologies.

[29] DOĞAN, F., DEHGHANPOUR, H., SUBAŞI, S., & MARAŞLI, M. (2022). Characterization of carbon fiber reinforced conductive mortars filled with recycled ferrochrome slag aggregates. Journal of Sustainable Construction Materials and Technologies, 7(3), 145–157.

[30] Marasli, M., Subasi, S., & Dehghanpour, H. (2022). Development of a maturity method for GFRC shell concretes with different fiber ratios. European Journal of Environmental and Civil Engineering, 26(15).

[31] SUBASI, S., DEHGHANPOUR, H., & MARASLI, M. (2022). Production and Characterization of GRC-SWCNT Composites for Shell Elements. Materials Science.

[32] DEHGHANPOUR, H., & YILMAZ, K. (2020). Heat Behavior of Electrically Conductive Concretes with and without Rebar Reinforcement. Materials Science, 26(4), 471–476.

[33] El-Dieb, A. S., El-Ghareeb, M. A., Abdel-Rahman, M. A. H., & Nasr, E. S. A. (2018). Multifunctional electrically conductive concrete using different fillers. Journal of Building Engineering, 15(June 2017), 61–69.

[34] ASTM C597. (2009). Standard test method for pulse velocity through concrete. American Society for Testing and Materials.

[35] ASTM C215. (2019). Standard Test Method for Fundamental Transverse, Longitudinal, and Torsional Resonant Frequencies of Concrete Specimens. American Society for Testing and Materials.

[36] ASTM A956. (2006). Standard Test Method for Leeb Hardness Testing of Steel Products. American Society for Testing and Materials.

[37] TS EN 196-1. (2005). Methods of testing cement–Part 1: Determination of strength. Turkish Standard.

[38] Dehghanpour, H., Yilmaz, K., Afshari, F., & Ipek, M. (2020). Electrically conductive concrete: A laboratory-based investigation and numerical analysis approach. Construction and Building Materials, 260, 119948.

[39] Tian, J., Fan, C., Zhang, T., & Zhou, Y. (2019). Rock breaking mechanism in percussive drilling with the effect of high-frequency torsional vibration. Energy Sources, Part A: Recovery, Utilization and Environmental Effects, 0(00), 1–15.

[40] Luo, J., Duan, Z., Xian, G., Li, Q., & Zhao, T. (2015). Damping Performances of Carbon Nanotube Reinforced Cement Composite. Mechanics of Advanced Materials and Structures, 22(3), 224–232.

[41] Dehghanpour, H., Subasi, S., Guntepe, S., Emiroglu, M., & Marasli, M. (2022). Investigation of fracture mechanics, physical and dynamic properties of UHPCs containing PVA, glass and steel fibers. Construction and Building Materials, 328, 127079.

[42] Kabirova, A., Uysal, M., Hüsem, M., Aygörmez, Y., Dehghanpour, H., Pul, S., & Canpolat, O. (2022). Physical and mechanical properties of metakaolin-based geopolymer mortars containing various waste powders. European Journal of Environmental and Civil Engineering, 1–20.

[43] Song, Z., Xue, X., Li, Y., Yang, J., He, Z., Shen, S., … Zhang, N. (2016). Experimental exploration of the waterproofing mechanism of inorganic sodium silicate-based concrete sealers. Construction and Building Materials, 104, 276–283.

[44] Gomez-Heras, M., Benavente, D., Pla, C., Martinez-Martinez, J., Fort, R., & Brotons, V. (2020). Ultrasonic pulse velocity as a way of improving uniaxial compressive strength estimations from Leeb hardness measurements. Construction and Building Materials, 261, 119996.

[45] García-Del-Cura, M. Á., Benavente, D., Martínez-Martínez, J., & Cueto, N. (2012). Sedimentary structures and physical properties of travertine and carbonate tufa building stone. Construction and Building Materials, 28(1), 456–467.

[46] Dehghanpour, H., Doğan, F., & Yılmaz, K. (2022). Development of CNT–CF–Al2O3-CMC gel-based cementitious repair composite. Journal of Building Engineering, 45, 103474.

[47] Kang, J., & Al-sabah, S. (2020). Effect of Single-Walled Carbon Nanotubes on Strength Properties of Cement Composites. Materials, 1–21.

[48] Musso, S., Tulliani, J. M., Ferro, G., & Tagliaferro, A. (2009). Influence of carbon nanotubes structure on the mechanical behavior of cement composites. Composites Science and Technology, 69(11–12), 1985–1990.

[49] Saleh, N. J., Ibrahim, R. I., & Salman, A. D. (2015). Characterization of nano-silica prepared from local silica sand and its application in cement mortar using optimization technique. Advanced Powder Technology, 26(4), 1123–1133.

[50] Huynh, T.-V., Seo, Y., & Lee, D. (2021). The Effect of Silica Sand Proportion in Laser Scabbling Process on Cement Mortar. Metals, 11(12), 1914.

[51] Mousavi, M. A., & Bahari, A. (2019). Influence of functionalized MWCNT on microstructure and mechanical properties of cement paste. Sādhanā, 44(5), 103.